# High voltage vacuum-deposited $CH_3NH_3PbI_3$-$CH_3NH_3PbI_3$ tandem solar cells

Jorge Avila,[a] Cristina Momblona,[a] Pablo Boix, [a] Michele Sessolo,[a] Miguel Anaya,[b] Gabriel Lozano, [b] Koen Vandewal,[c] Hernán Míguez[b] and Henk J. Bolink*[a]

[a] Instituto de Ciencia Molecular, Universidad de Valencia, C/ J. Beltrán 2, 46980, Paterna, Spain

[b] Institute of Materials Science of Seville, Spanish National Research Council-University of Seville, C/Américo Vespucio 49, 41092, Seville, Spain.

[c] Institute for Materials Research (IMO-IMOMEC), Universiteit Hasselt, Wetenschapspark 1, 3590 Diepenbeek, Belgium

**Supporting Information**

Materials. Photolithographically patterned ITO coated glass substrates were purchased from Naranjo Substrates (www.naranjosubstrates.com). 2,2'-(Perfluoronaphthalene-2,6-diylidene) dimalononitrile ($F_6$-TCNNQ), N4,N4,N4",N4"-tetra([1,1'-biphenyl]-4-yl)-[1,1':4',1"-terphenyl]-4,4"-diamine (TaTm) and N1,N4-bis(tri-p-tolylphosphoranylidene)benzene-1,4-diamine (PhIm) were provided from Novaled GmbH. Fullerene ($C_{60}$) was purchased from sigma Aldrich. $PbI_2$ was purchased from Tokyo Chemical Industry CO (TCI), and $CH_3NH_3I$ (MAI) from Lumtec**.** $TiO_2$ nanoparticle suspensions were prepared in IMEC and deposited through a low temperature process compatible with ITO substrates. Non-aqueous sol-gel route is used,[1] in which the oxygen required for the nanoparticle formation is provided by benzyl alcohol. In detail, 2 mL anhydrous ethanol is mixed with 0.5 mL titanium (IV) chloride ($TiCl_4$ from Sigma Aldrich) inside a nitrogen field glove box. After stirring for 10 minutes at room temperature, 10 mL benzyl alcohol (Sigma Aldrich) is added to the mixture leading to a light yellow and clear solution. This solution is stirred for at least 18 hours at 80 ºC leading to colourless hazy suspension. The haziness of the suspension is caused by creation of white titanium oxide nanoparticles. To separate them, 1 mL of the resulting

milky suspension was precipitated in 10 mL of diethyl ether (from Sigma Aldrich) and centrifuged at 5000 rpm for two minutes to isolate the nanoparticles from the solvent and the unreacted precursor. After centrifuge, the solvent was drained out and solid white nanoparticles were dispersed into 3 mL pure ethanol leading to milky (white and hazy) solution. To stabilize this final dispersion, 45 µL Diisopropoxytitaan-bis-(acetylacetonaat) (TiAcac purchased from Sigma Aldrich) is added to the solution. After less than one hour, a light green and clear solution is created.[2] This is the final product containing of $TiO_2$ nanoparticles in pure ethanol.

Device preparation. ITO-coated glass substrates were subsequently cleaned with soap, water and isopropanol in an ultrasonic bath, followed by UV-ozone treatment. The $TiO_2$ dispersion was deposited in air by spin-coating at 3000 rpm for 30 s and annealed at 100 ºC for 30 min, leading to a 20-40 nm thick compact layer. Them, they were transferred to a vacuum chamber integrated into a nitrogen-filled glovebox (MBraun, $H_2O$ and $O_2 < 0.1$ ppm) and evacuated to a pressure of $1 \cdot 10^{-6}$ mbar. The vacuum chamber uses a turbomolecular pump (Pfeiffer TMH 261P, DN 100 ISO-K, 3P) coupled to a scroll pump. The vacuum chamber is equipped with six temperature controlled evaporation sources (Creaphys) fitted with ceramic crucibles. The sources were directed upwards with an angle of approximately 90º with respect to the bottom of the evaporator. The substrate holder to evaporation sources distance is approximately 20 cm. Three quartz crystal microbalance (QCM) sensors are used, two monitoring the deposition rate of each evaporation source and a third one close to the substrate holder monitoring the total deposition rate. For thickness calibration, we first individually sublimed the charge transport materials and their dopants (TaTm and $F_6$-TCNNQ, $C_{60}$ and PhIm). A calibration factor was obtained by comparing the thickness inferred from the QCM sensors with that measured with a mechanical profilometer (Ambios XP1). Then these materials were co-sublimed at temperatures ranging from 135-160 ºC for the dopants to 250 ºC for the pure charge transport molecules, and the evaporation rate was controlled by separate QCM sensors and adjusted to obtain the desired doping concentration. In general, the deposition rate for TaTm and $C_{60}$ was kept constant at 0.8 Å $s^{-1}$ while varying the deposition rate of the dopants during co-deposition. Pure TaTm, $F_6$-TCNNQ, BCP and $C_{60}$ layers were deposited at a rate of 0.5 Å $s^{-1}$.

After deposition of the $TiO_2$, 10 nm thick $C_{60}$ is vacuum-deposited. Once completed this deposition, the chamber was vented with dry $N_2$ to replace the ETL crucible with those

containing the starting materials for the perovskite deposition, $PbI_2$ and $CH_3NH_3I$. The vacuum chamber was evacuated again to a pressure of $10^{-6}$ mbar, and the perovskite films were then obtained by co-deposition of the two precursors. The calibration of the deposition rate for the $CH_3NH_3I$ was found to be difficult due to non-uniform layers and the soft nature of the material which impeded accurate thickness measurements. Hence, the source temperature of the $CH_3NH_3I$ was kept constant at 70 ºC and the $CH_3NH_3I$:$PbI_2$ ratio was controlled off line using grazing incident x-ray diffraction by adjusting the $PbI_2$ deposition temperature. The optimum deposition temperatures were found to be 250 ºC for the $PbI_2$ and 70 ºC for the $CH_3NH_3I$. After deposition of the desired thickness perovskite film, the chamber was vented, and the crucibles replaced with those containing the hole-transport materials and evacuated again to a pressure of $10^{-6}$ mbar. Then, a film of pure TaTm (10 nm) follows by 25 nm of the p-doped hole-transport layer (TaTm: $F_6$-TCNNQ) was evaporated. For the reference Front Cell device, the metal top contact (Au, 100 nm thick) was deposited. In the case of tandem devices, 25 nm of the n-doped electron-transport layer ($C_{60}$: PhIm) capped with 10 nm of the pure $C_{60}$ were deposited to complete the charge recombination layers. Once completed this deposition, the chamber was vented with dry $N_2$ to replace the ETL crucibles with those containing the starting materials for the perovskite deposition, $PbI_2$ and $CH_3NH_3I$. Following the previous described protocol, the back subcell perovskite layer was deposited. After deposition of the desired thickness perovskite film, the chamber was vented, and the crucibles replaced with those containing the hole-transport materials and evacuated again to a pressure of $10^{-6}$ mbar. Then, a film of pure TaTm (10 nm) follows by 40 nm of the p-doped hole-transport layer (TaTm: $F_6$-TCNNQ) was evaporated. Afterwards the metal top contact (Au, 100 nm thick) was deposited.

Characterization. Absorption spectra were collected using a fiber optics based Avantes Avaspec2048 Spectrometer. Characterization of the solar cells was performed as follows. The external quantum efficiency (EQE) was estimated using the cell response at different wavelength (measured with a white light halogen lamp in combination with band-pass filters), where the solar spectrum mismatch is corrected using a calibrated Silicon reference cell (MiniSun simulator by ECN, the Netherlands). The current density-voltage (J-V) characteristics were obtained using a Keithley 2400 source measure unit and under white light illumination, and the short circuit current density was corrected considering the device EQE. The electrical characterization was validated using a solar simulator by

Abet Technologies (model 10500 with an AM1.5G xenon lamp as the light source). Before each measurement, the exact light intensity was determined using a calibrated Si reference diode equipped with an infrared cut-off filter (KG-3, Schott). The J-V curves were recorded between -0.2 and 2.4 V with 0.01 V steps, integrating the signal for 20 ms after a 10 ms delay. This corresponds to a speed of about 0.3 V $s^{-1}$. The layout used to test the solar cells has four equal areas (0.04 $cm^2$, defined as the overlap between the ITO and the top metal contact) and measured through a shadow mask with 0.01 $cm^2$ aperture.

**Optics**

We have performed a spectroscopic analysis of the light reflected and transmitted by the samples. In particular, specular reflectance and ballistic transmittance at three different angles of the incident light beam, i.e. 6º, 30º, and 50º, for s and p polarized light, were experimentally obtained.

Based on this characterization we extract the real (n) and imaginary (k) parts of the complex refractive index of the films. We have developed a homemade code based on the transfer matrix method to model the evaporated film considering air as the incoming and outgoing media and two layers: i) a perovskite (or ESL, or HTL) film, and ii) a 1mm-thick (0.74 mm for ESL, HTL) glass substrate. The high optical quality of the analysed samples indicates that the different interfaces can be considered as plane-parallel. We use a Forouhi-Bloomer model to extract the complex refractive index of the materials.[3] This model considers a nanocrystalline semiconductor, which is ideal for the materials that we have studied. In particular, we have used the Jobin Yvon (new amorphous) parametrization[4]

$$n(E) = n_\infty \sum_{j=1}^{N} \frac{B_j\left(E - E_j\right) + C_j}{(E - E_j)^2 + \Gamma_j^2}, \tag{1}$$

$$k(E) = \begin{cases} \sum_{j=1}^{N} \frac{f_j (E - E_g)^2}{(E - E_j)^2 + \Gamma_j^2}; \text{for } E > E_g \\ 0; \text{for } E < E_g \end{cases} \tag{2}$$

with

$$B_j = \frac{f_j}{\Gamma_j}\left(\Gamma_j^2 - \left(E - E_j\right)^2\right) \text{ and } C_j = 2f_j\Gamma_j\left(E - E_j\right)$$

Where $E$ is the energy, $E_g$ is the bandgap, and $E_j$, $f_j$, and $\Gamma_j$ are the position, strength, and width of one oscillator. In our case, we have employed 3 oscillators (N=3). Please note that this formalism is fully consistent with Kramers-Kronig relations

$$n(\omega) = n_0 + \frac{2}{\pi}\mathrm{P}\int_0^\infty \frac{\Omega k(\Omega)}{\Omega^2 - \omega^2}\, d\Omega, \qquad (3)$$

where $\omega = 2\pi c/\lambda$ is the angular frequency and $c$ is the speed of light in vacuum.

Then, we employ a genetic algorithm to simultaneously fit the p and s polarizations of the angular dependence of specular reflectance and ballistic transmittance spectra for the different films provided. Full details on the model can be found elsewhere.[5, 6]

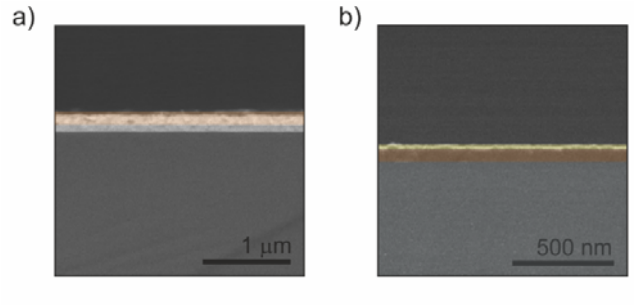


**Figure S1.** Zoom out of a scanning electron microscopy image of a cross section of an evaporated $CH_3NH_3PbI_3$ perovskite film (a) and a $C_{60}$ film (b).

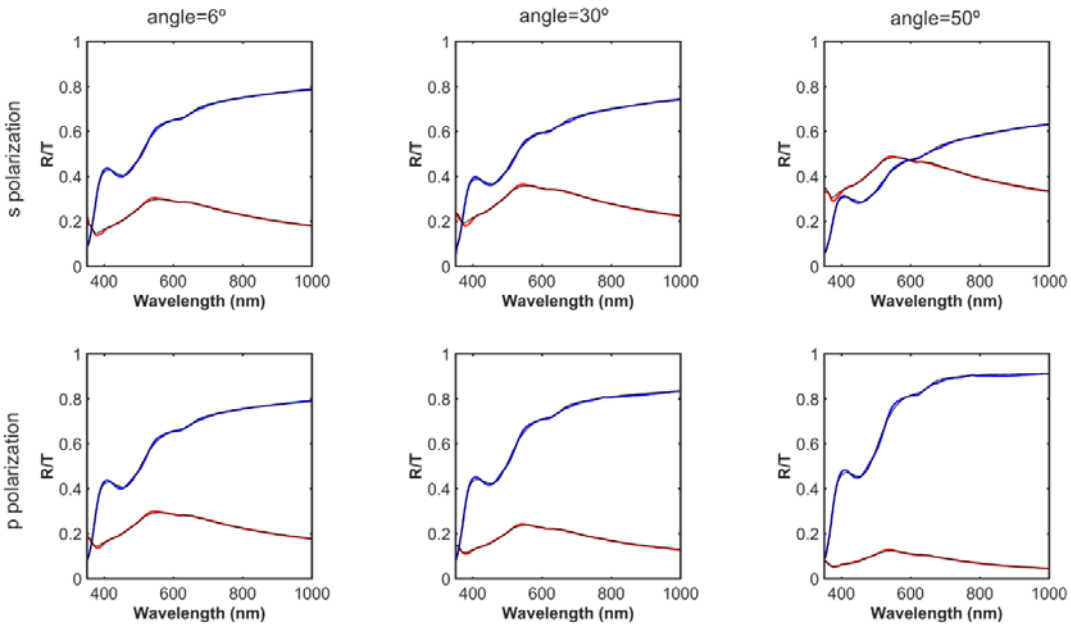


**Figure S2.** Experimental (colour lines) and calculated (black lines) reflectance and transmittance spectra of an evaporated 65 nm-thick $C_{60}$ film on glass. S and p polarization are shown in the top and bottom panels, respectively. The angle of the incident light beam is set at 6°, 30°, and 50°.

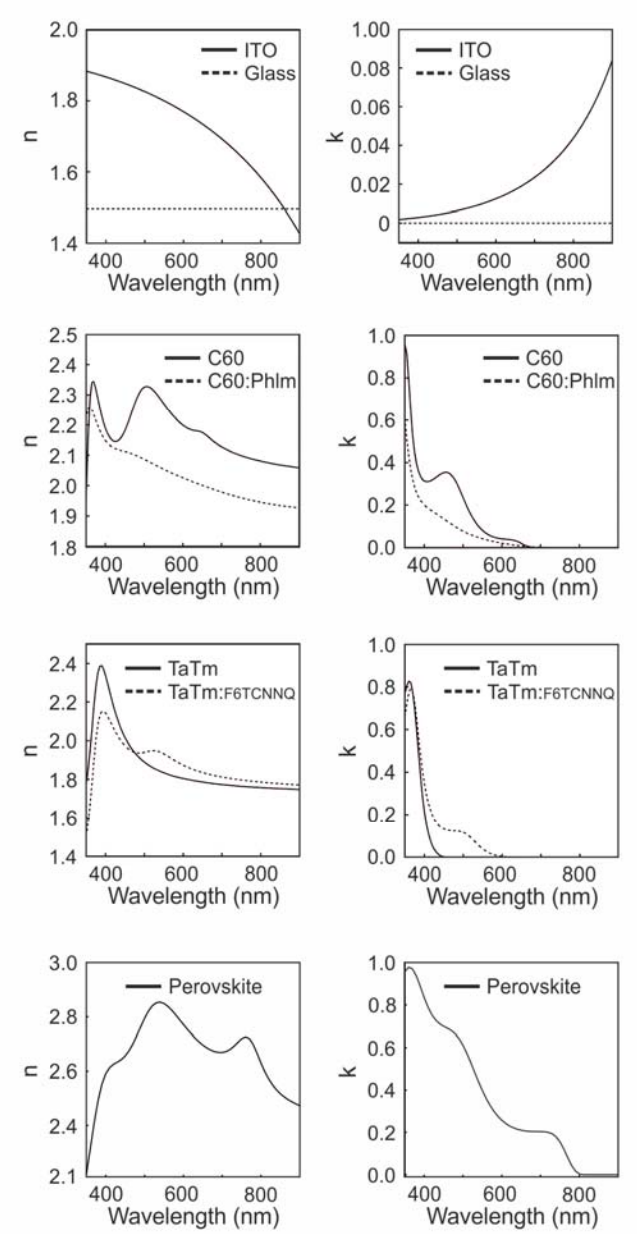


**Figure S3.** Refractive indices for the different materials comprising the tandem device. We have taken the n and k values from the literature for gold[7] and $TiO_2$.[8]

**C60**

**Table S1.** Optical model parameters attained for the intrinsic and doped $C_{60}$ films.

| Parameter | $C_{60}$ | $C_{60}$: PhIm (60 wt%) |
|---|---|---|
| **Eg (eV)** | 1.78 | 1.68 |
| **$n_\infty$** | 1.91 | 1.83 |
| **$f_1$** | 0.011 | 0.042 |
| **$f_2$** | 0.055 | 0.024 |
| **$f_3$** | 0.009 | 0.010 |
| **$E_1$ (eV)** | 1.91 | 1.80 |
| **$E_2$ (eV)** | 2.55 | 2.73 |
| **$E_3$ (eV)** | 3.52 | 3.65 |
| **$\Gamma_1$ (eV)** | 0.100 | 0.584 |
| **$\Gamma_2$ (eV)** | 0.347 | 0.581 |
| **$\Gamma_3$ (eV)** | 0.181 | 0.246 |
| **d (nm)** | 67 | 33 |

Please notice the reliability of our method since profilometer measurements give a thickness of 65 nm (35 nm) for the intrinsic (doped) $C_{60}$, while calculations yield 67 nm (33 nm).

**TaTm**

**Table S2.** Optical model parameters attained for the intrinsic and doped TaTm films.

| Parameter | TaTm | TaTm: $F_6$-TCNNQ (11 wt%) |
|---|---|---|
| **Eg (eV)** | 2.69 | 1.92 |
| **n** | 1.66 | 1.65 |
| **$f_1$** | 0.146 | 0.028 |
| **$f_2$** | 0.014 | 0.027 |
| **$E_1$ (eV)** | 3.30 | 3.34 |
| **$E_2$ (eV)** | 2.89 | 2.37 |
| **$\Gamma_1$ (eV)** | 0.280 | 0.282 |
| **$\Gamma_2$ (eV)** | 0.340 | 0.260 |
| **d (nm)** | 47 | 34 |

Profilometer measurements give a thickness of 40 nm (40 nm) for the intrinsic (doped) TaTm while calculations yield 47 nm (34 nm).

**$CH_3NH_3PbI_3$**

In the case of perovskite films, first we have confirmed the high optical quality of the films as it is a recurrent problem in the literature. In order to do that, we have measured total reflectance, diffuse reflectance, total transmittance and diffuse transmittance with an integrating sphere. These measurements allow us to determine the fraction of incident light absorbed by the films as shown in Figure S4a. Besides, the diffuse reflectance spectra reveal the high optical quality of the thin films due to the negligible fraction of diffusely scattered light (see Figure S4b).

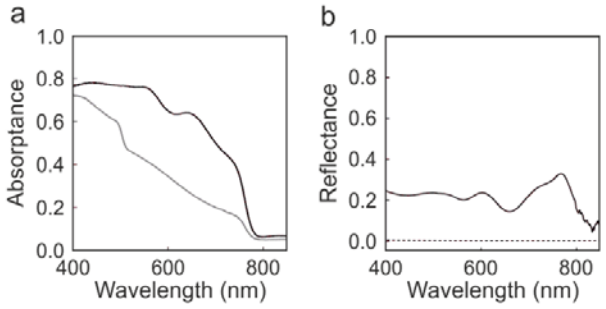


**Figure S4.** (a) Experimental absorptance spectra of co-evaporated perovskite films with thicknesses of 490 nm (black) and 120 nm (grey). A=1-R-T. (b) Experimental total (solid black) and diffuse (dashed black) reflectance spectra of a co-evaporated perovskite film of 490 nm of thickness.

**Table S3.** Optical model parameters attained for the perovskite films.

| **Parameter** | **Thick film $CH_3NH_3PbI_3$** |
|---|---|
| **Eg (eV)** | 1.53 |
| **n** | 2.16 |
| **$f_1$** | 0.1285 |
| **$f_2$** | 0.089 |
| **$f_3$** | 0.051 |
| **$E_1$ (eV)** | 1.60 |
| **$E_2$ (eV)** | 2.40 |
| **$E_3$ (eV)** | 3.30 |
| **$G_1$ (eV)** | 0.100 |
| **$G_2$ (eV)** | 0.432 |
| **$G_3$ (eV)** | 0.548 |
| **d (nm)** | 91 |

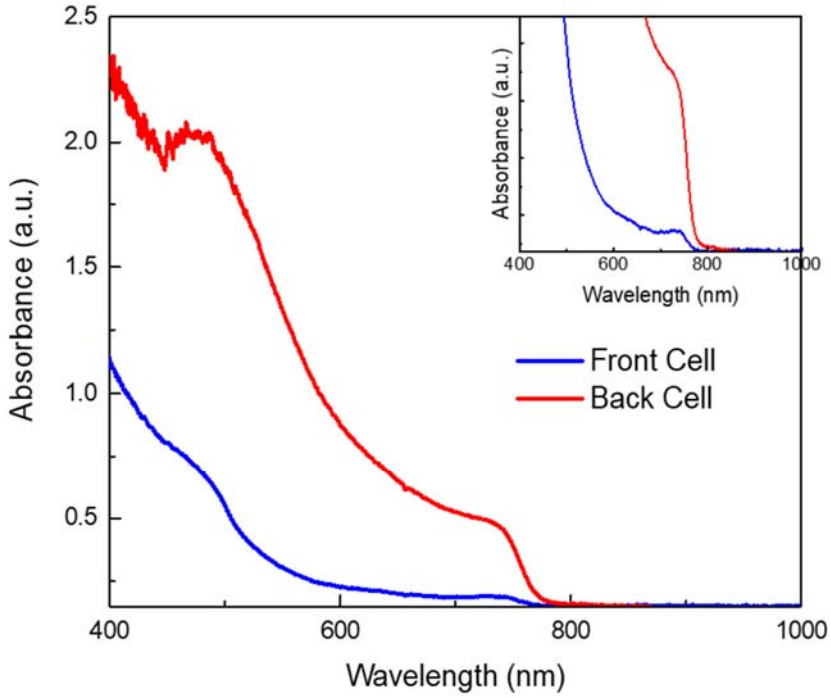


**Figure S5.** Perovskite absorbance spectra of front cell (90 nm) and back cell (400 nm). The inset is a zoom of the absorption onset.

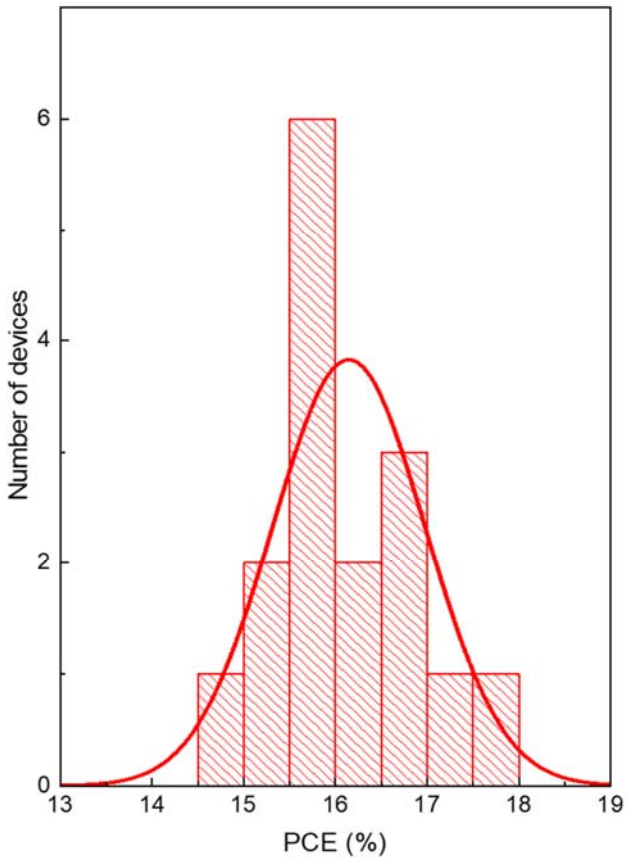


**Figure S6.** PCE statistical distribution of tandem devices. Solid line represents the Gaussian distribution fitting for the PCE.

**Table S4.** Statistical distribution of J-V parameters of devices measured under standard AM1.5G illumination.

| $V_{oc}$ (V) | $J_{sc}$ (mAcm$^{-2}$) | FF (%) | PCE (%) |
|---|---|---|---|
| 2.25 ± 0.04 | 8.6 ± 0.4 | 83 ± 1 | 16.1 ± 0.8 |

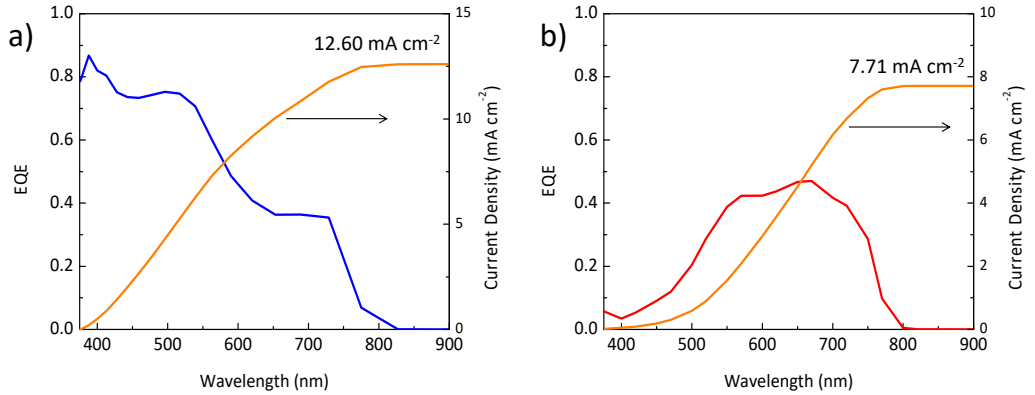


**Figure S7.** EQE spectra for the single junction (a) front cell and (b) back cell filtered with the front perovskite film.

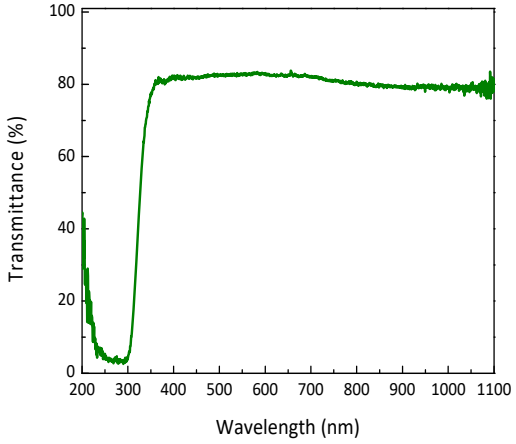


**Figure S8.** Transmittance spectrum of the glass substrate for the perovskite film used to filter the back cell (see Fig. S7).

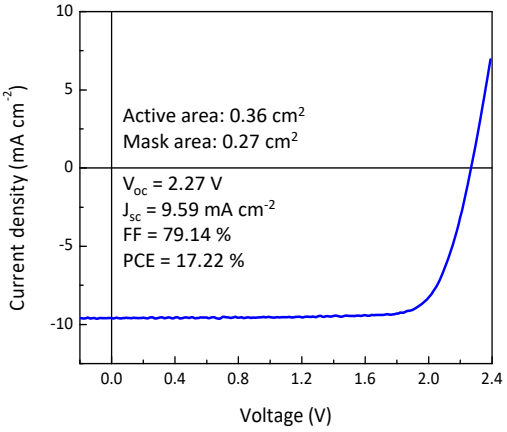


**Figure S9.** J-V characteristics under 100 mW/cm$^2$ illumination for a homojunction tandem solar cell with an active area of 0.36 cm2 and a mask area of 0.27 cm$^2$.

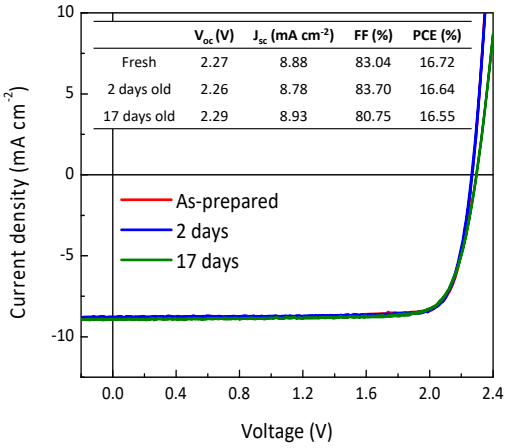


**Figure S10.** J-V characteristics under 100 mW/cm$^2$ illumination for a homojunction tandem solar cell over time. The device was kept in nitrogen in between measurements.

## References


1. M. Niederberger, *Accounts of Chemical Research*, 2007, **40**, 793-800.
2. A. Hadipour, Doped titanate. WO 2017/108710 A1, June 29th 2017.
3. A. R. Forouhi and I. Bloomer, *Physical Review B*, 1986, **34**, 7018-7026.

4. J. Yvon, New Amorphous Dispersion Formula, http://www.horiba.com/fileadmin/uploads/Scientific/Downloads/OpticalSchool_CN/TN/ellipsometer/New_Amorphous_Dispersion_Formula.pdf.
5. M. Anaya, J. P. Correa-Baena, G. Lozano, M. Saliba, P. Anguita, B. Roose, A. Abate, U. Steiner, M. Gratzel, M. E. Calvo, A. Hagfeldt and H. Miguez, *Journal of Materials Chemistry A*, 2016, **4**, 11214-11221.
6. Forouhi-Bloomer alias Amorphous Dispersion Formula, http://www.horiba.com/fileadmin/uploads/Scientific/Downloads/OpticalSchool_CN/TN/ellipsometer/Forouhi-Bloomer_alias_Amorphous_Dispersion_Formula.pdf.
7. S. Babar and J. H. Weaver, *Appl. Opt.*, 2015, **54**, 477-481.
8. J. S. Alberto, A. Miguel, C. M. E., A. C. Mercedes, A. Carlos, G. Elena, M. Noelia, G. Manuel, P. Thomas, E. G. Ramón and M. Hernán, *Advanced Optical Materials*, 2017, **5**, 1600833.